ChemComm

Cite this: *Chem. Commun.*, 2012, **48**, 3599–3601

www.rsc.org/chemcomm

COMMUNICATION

Investigation of encapsulation of insulin biotemplate within *C*-methylresorcin[4]arenes†

Harshita Kumari,[a] Steven R. Kline[b] and Jerry L. Atwood*[a]

Received 25th December 2011, Accepted 28th January 2012
DOI: 10.1039/c2cc18071e

Solution structure of insulin templated *C*-methyl resorcin[4]arene nanocapsules has been investigated using neutron scattering. The insulin biotemplate has enhanced the limits of encapsulation and enabled formation of a larger spherical molecular host.

The investigation of biomolecules as templates is a significant area of endeavour. Biomolecules such as tobacco mosaic virus (TMV) and ferritin serve as templates for fabrication of metal-oxide nanotubes and thin layer structures.[1] TMV has a 300 nm long tubular structure with a hollow diameter of about 4 nm. These tubular structures have the potential to aggregate in a head to tail or side-by-side fashion to form either 2-D or 3-D structures.[2–4] Insulin fibrils[5] and insulin amyloid[6] superstructures act as biotemplates for gold nanoparticle chains[5] and nanopatterns in gold layers,[6] respectively. One of the major advantages of using biotemplates is that they allow manipulations under ambient conditions.

Inspired by nature's exquisite collection of self-assembled biomolecules and its close association with supramolecular chemistry, we explored humalog insulin (commercially available)[7–14] as a biotemplate for resorcin[4]arene-based (Rs) nanoassemblies. The advent of hexameric nanocapsules dates to 1997, with the formation of the 72-hydrogen-bonded self-assembly of six RsC*n* (where $n = 1$ and represent alkyl chain) and eight water molecules with an internal volume of $\sim$1500 Å^3.[15,16] Later, structurally similar pyrogallol[4]arenes (PgC*n*) were shown to self-assemble as hexamers with an enclosed space of $\sim$1250 Å^3.[17] Pyrogallol[4]arene hexamers were further explored for guest encapsulation using fluorescent molecular probes such as pyrene butyric acid (PBA),[18] and ADMA.[19] Likewise, dianionic guests with tetracation calix[4]arene[20,21] and C_{70} with t-Bu-calix[6]arene[22] are excellent examples of host–guest complexes.

In the current study, we have utilized humalog insulin as a biotemplate for resorcin[4]arene (Rs) macrocycles to investigate the possibility of panelling the macrocycles onto the insulin moiety, thereby effectively constructing larger hosts. Given the complexity of protein crystallization with organic molecules, we studied these nanoassemblies in solution. We employed the small-angle neutron scattering (SANS) technique in order to probe the solution geometry of the assembly.

SANS measurements for this study of ReC_1-insulin complexes were designed on the contrast variation method wherein we examine the inhomogeneities in solution, which refers to the differences in the scattering length densities (SLDs) of the solute and the solvent phases that provide contrast between the two phases. For these experiments, we prepared acetone-water based solvent systems with SLDs (Å^{-2}) of 3.7×10^{-6}, 5.0×10^{-6} and 6.7×10^{-6}. This increment and differences in SLDs were obtained by enhanced deuteration. Samples of 0.1 mol L^{-1} RsC_1 (a-1, a-2, a-3), humalog insulin (b-1, b-2, b-3) and RsC_1 with humalog insulin/$RsC_1 \subset$ Insulin (1 equiv. of a and b each; c-1, c-2, c-3)[14] were the prepared in the three solvents (1–3). A matrix of sample-solvent systems was thus created for each species (Table 1). For $RsC_1 \subset$ Insulin samples, a molar ratio of 56 : 1 for RsC_1 : Insulin (c-1, c-2, c-3) was maintained to ensure the presence of sufficient amount of macrocycle to enable templation around insulin.

The SANS measurements were conducted at RT on NG7 30 m SANS instrument at the NIST Center for Neutron Research (NCNR-NIST), Gaithersburg, MD, USA,[24] and the data analyses was performed on Igor Pro.[25] First, the SANS measurements were conducted on control samples (blank solutions of solvent)[26,27] to investigate the presence of self-assembled entities. The data analyses for control samples gave sufficient statistics for Schulz sphere fit and indicated the presence of a spherical entities of radius (5.9–7.0) Å.[14] These spherical clusters suggest association of acetone molecules

Table 1 Sample-solvent SLD matrix of SANS insulin-ReC_1 experiments. Each sample of ReC_1, insulin and $ReC_1$with insulin was prepared in three solvent systems (3 SLDs)

S. No.	Sample (solute)	SLD solvent (Å^{-2})
a-1	ReC_1	3.70×10^{-06}
a-2	ReC_1	6.36×10^{-06}
a-3	ReC_1	5.00×10^{-06}
b-1	Insulin	3.70×10^{-06}
b-2	Insulin	6.36×10^{-06}
b-3	Insulin	5.00×10^{-06}
c-1	ReC_1 + Insulin	3.70×10^{-06}
c-2	ReC_1 + Insulin	6.36×10^{-06}
c-3	ReC_1 + Insulin	5.00×10^{-06}

[a] *Department of Chemistry, University of Missouri-Columbia, 601 S. College Avenue, Columbia, MO 65211, USA. E-mail: AtwoodJ@missouri.edu; Fax: +1 573 882 2754; Tel: +1 573 882 8374*
[b] *NIST Center for Neutron Research, Gaithersburg, MD 20899-6102, USA*
† Electronic supplementary information (ESI) available. See DOI: 10.1039/c2cc18071e

with H_2O or D_2O in solution to form weak micellar species. On the other hand, the scattering data for RsC_1 (a-1, a-2, a-3) were fitted to both Schulz sphere and bimodal Schulz sphere models.[26,27] The data analysis for the bimodal Schulz sphere model of RsC_1 was statistically superior to a single mode, and thus revealed the presence of spheres of radius 7 Å and 10 Å.[14] Given the structural similarity between PgC*n* and RsC*n* nanocapsules[15,17] and improved scattering statistics obtained for the bimodal Schulz sphere fit, the SANS data analyses indicate the presence of hydrogen-bonded RsC_1 dimer (7 Å) and hexamer (10 Å) in solution.[28]

An overlay of neutron scattering curves for RsC_1 (a-2) and insulin (b-2) suggest differences at both low and high q values (Fig. 2). Differences in scattering curves indicate the presence of other geometric species for insulin in solution. Hence, the scattering data of insulin was fitted to spherical, cylindrical and ellipsoidal models. The scattering data of insulin at all solvent SLDs yielded best statistics for a bimodal Schulz sphere fit (b-1, b-2, b-3). This model demonstrated the presence of two spherical entities with the sizes of radius ~10 Å and ~25 Å.[14]

In the earlier reported SANS studies on insulin by Krueger and co-workers, the theoretical dimeric (cylinder) dimensions of insulin were calculated to yield 42 Å length and 22 Å diameter.[29] However, the theoretical dimensions in solution converged to a R_g (radius of gyration) of 14.4 Å from a Gunier plot.[29] In solution, Krueger *et al.* measured values depending on the contrast, and obtained slightly smaller R_g in D_2O. For the Guinier plot, we only extract the initial slope of the data, with no assumptions about the shape. Then to convert the R_g into a sphere radius R to compare to our SANS fits, we adjust our fitted sphere radius using the definition (R_g = 0.77*R), to get radius values comparable to the earlier reported SANS insulin dimensions.[29] Thus for a dimeric insulin molecule of 14.4 Å (Guinier plot), we would get a corresponding radius of 18.7 Å (Schulz sphere model). SANS data analyses of humalog insulin fitted to bimodal Schulz sphere yields spheres of radius 10 Å and 25 Å that corresponds to a monomer and a trimer of insulin, respectively. These values are similar for all three solvent systems (b-1, b-2, b-3); however some of the data points at low q values indicate protein aggregation and hence these data are not included in the fitted curve.[14]

Comparing the scattering data analyses of insulin with those of RsC_1 show the radius of an insulin monomer close to that of a hydrogen-bonded RsC_1 hexamer. Note the difference between the size of an insulin monomer (~10 Å) and a trimer (~25 Å) is about ~15 Å. This information is critical in identifying species beyond and between the radii limits. While the scattering curves of insulin and RsC_1 appear widely different, the SANS data for RsC_1⊂Insulin indicate the absence of very large assemblies (~25 Å) at low q. This can be inferred from the difference in scattering curves for RsC_1⊂Insulin and RsC_1 at low q values that suggest distinct structural differences (Fig. 2).

The scattering curves for RsC_1⊂Insulin (c-1, c-2, c-3) were fitted to bimodal Schulz sphere model. The data analyses at varying solute SLDs indicate the presence of two spherical entities of radius ~10 Å and ~16 Å that correspond to RsC_1 hexamer or insulin monomer and RsC_1⊂Insulin monomer, respectively.

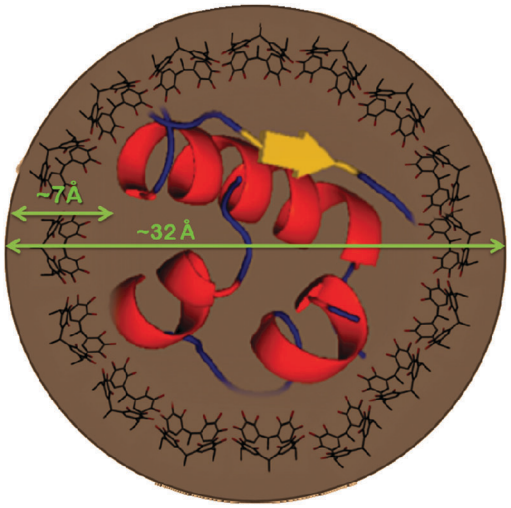

Fig. 1 A model of insulin monomer[23] within pyrogallol[4]arene macrocycles in solution. This model of spherical nanoassembly (~32 Å) shows panelling of macrocyle[16] (~7 Å) around insulin template[a] (~19 Å). The surface of insulin is primarily hydrophilic; however, it has a hydrophobic center.

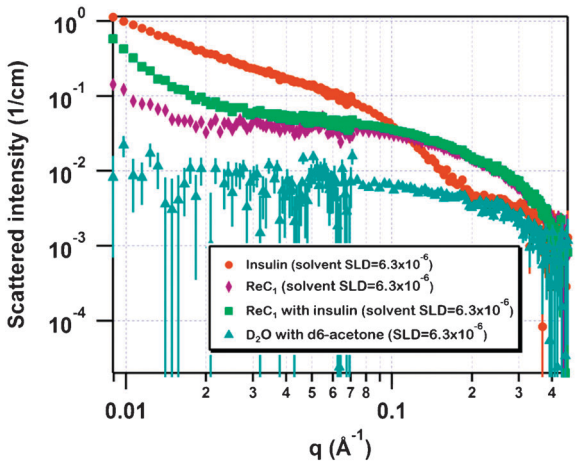

Fig. 2 Small-angle neutron scattering curves of insulin (b-2; brown circles), *C*-methylresorcin[4]arene (a-2; purple diamond), insulin with *C*-methylresorcin[4]arene (c-2; green squares) and D_2O with d6-acetone (turquoise triangles). Error bars on the data points represent one standard deviation of the intensity. 'q' is the scattering vector'.

The SANS data for typical PgC_3/RsC_3 and PgC_1/RsC_1 dimers fit to a polydisperse sphere,[27,30] of radius ≈7 Å and ≈6.8 Å, respectively.[31] These solution phase measurements are in agreement with the previously reported XRD structures that demonstrate the stability of these nanocapsules in solution.[28,31,32] Clearly, the bowl size of a single RsC_1 (6.8 Å) matches with the shell size observed for RsC_1⊂Insulin (Fig. 1).[14] Calculating the shell volume for this larger assembly (16 Å) using eqn (1), yields the V_{shell} of ≈15 700 Å^3 for nRsC_1s.

$$V_{shell} = (4/3)\pi((R_{insulin} + RsC_1)^3 - R_{insulin}^3) \quad (1)$$

Thus, the difference of 15 700 Å^3 corresponds to the volume of 24 bowls of RsC_1 (each bowl ≈ 659 Å^3). For each RsC_1⊂Insulin data analysis, the two solute SLDs were fixed to that of RsC_1 hexamer and nRsC_1⊂Insulin monomer.

The solute SLD for $nRsC_1 \subset$Insulin monomer was varied from 2.03×10^{-6} Å^{-2} to 2.08×10^{-6} Å^{-2} for n = 8 to n = 24. A range of macrocyclic units (8–24) were employed for data analyses to estimate the differences in scattering statistics and presence of multiple species. The upper limit of 24 for macrocycles was estimated from shell volume calculations. Interestingly, varying the macrocyclic number did not change the overall radius of RsC_1 (10 Å) and $nRsC_1 \subset$Insulin (16 Å).

As the solvent SLD increases from 3.7×10^{-6} Å^{-2} to 5.0×10^{-6} Å^{-2} to 6.3×10^{-6} Å^{-2}, the shell–solvent contrast or difference in SLDs increases from 1.62×10^{-6} Å^{-2}, 2.92×10^{-6} Å^{-2}, and 4.22×10^{-6} Å^{-2}, respectively. This difference in solvent–solute SLDs allows us to see the shell more clearly at a higher contrast. The data fitting for c-1 yields the radius of 15.97 Å that is smaller than expected insulin dimeric radius of 18.4 Å; however, the total spherical radius of 15.97 Å species corresponds to a core of monomeric insulin (10 Å) and a shell of (5.97 Å) RsC_1. An increase in shell size from 5.97 Å (c-1) to 6.7 Å (c-2) to 6.93 Å (c-3) is observed with an increase in contrast variation. The error bars, albeit small, account for the smaller difference in radius values for c-2 and c-3. Furthermore, the smoothness of the scattering curve at high q suggests, to some extent, the uniformity of the shell (24 RsC_1) around the insulin monomer; however, the smoothness of the shell cannot be quantified, given the surface roughness dimensions (small) that is not detectable by SANS at its high q limits. Given the possibility of presence of free (insulin/RsC_1) and bound (RsC_1 hexamer) species, it is difficult to quantify the amount of $RsC_1 \subset$Insulin formed. However, the volume fraction ratios of RsC_1 hexamer and $RsC_1 \subset$Insulin vary from 20 : 1 (c-1) to 17.9 : 1 (c-3) to 9 : 1 (c-2). This decrease in volume fraction ratios with an increase in contrast allows us to observe a higher volume fraction of $RsC_1 \subset$Insulin over RsC_1 hexamer. This study was repeated twice to confirm the reproducibility of self-assembled frameworks; within the error bars for c-2 and c-3, ($R \approx 16$ Å $\pm$ 1.0 Å) and thus confirms the presence of larger assemblies.[14]

Overall, humalog insulin has proved a useful biotemplate to construct molecular hosts in solution. SANS measurements reveal the encapsulation of monomeric insulin within hydrogen-bonded resorcin[4]arene nanocapsules. The suggested structure of the $RsC_1 \subset$Insulin nanocapsule has 8 to 24 arenes in a cone conformation (^{1}H NMR) providing possible interaction sites between opposite pyrogallols on the same arene.[14] This cone-shaped orientation of the macrocycle allows guest encapsulation and provides sufficient interaction sites between arenes and insulin surface that stitch the spheroidal assembly. In addition, the current study demonstrates the presence of a larger spherical resorcin[4]arene host (r = 16 Å) in solution with an internal volume more than thrice that of a hexamer and more than eleven times than that of a dimer. Clearly, the macrocycle is playing an important role in the formation of larger hosts and the self-assembly process is enabled by specific host–guest interactions. These results of SANS studies are intriguing because host–guest complexes thus formed not only extend the size of nanocapsules available as reaction vessels but also show that other geometric arrangements are possible for these macrocycles. Moreover, solution phase studies provide insight into systems that are difficult to crystallize.

We thank NSF for support of this work (J.L.A.). We thank the group of Prof. J. Tanner for help with protein assays. This work utilized facilities supported in part by the National Science Foundation under Agreement No. DMR-0944772 (S.R.K.). Certain trade names and company products are identified to adequately specify the experimental procedure. In no case does such identification imply recommendation or endorsement by the National Institute of Standards and Technology.

Notes and references

1 M. Knez, A. Kadri, C. Wege, U. Goesele, H. Jeske and K. Nielsch, *Nano Lett.*, 2006, **6**, 1172–1177.
2 K. Henrick and J. M. Thornton, *Trends Biochem. Sci.*, 1998, **23**, 358–361.
3 K. Namba, R. Pattanayek and G. Stubbs, *J. Mol. Biol.*, 1989, **208**, 307–325.
4 R. Pattanayek and G. Stubbs, *J. Mol. Biol.*, 1992, **228**, 516–528.
5 S. Hsieh and C.-w. Hsieh, *Chem. Commun.*, 2010, **46**, 7355–7357.
6 S. Wojcik, V. Babenko and W. Dzwolak, *Langmuir*, 2010, **26**, 18303–18307.
7 A. P. Ramirez, R. C. Haddon, O. Zhou, R. M. Fleming, J. Zhang, S. M. McClure and R. E. Smalley, *Science*, 1994, **265**, 84–86.
8 S. M. Biros and J. J. Rebek, *Chem. Soc. Rev.*, 2007, **36**, 93.
9 S. Liu and B. C. Gibb, *Chem. Commun.*, 2008, 3709.
10 Z. Laughrey and B. C. Gibb, *Chem. Soc. Rev.*, 2011, **40**, 363.
11 S. J. Dalgarno, N. P. Power and J. L. Atwood, *Coord. Chem. Rev.*, 2008, **252**, 825–841.
12 P. Jin, S. J. Dalgarno and J. L. Atwood, *Coord. Chem. Rev.*, 2010, **254**, 1760–1768.
13 J. Rebek, *Acc. Chem. Res.*, 2009, **42**, 1660–1668.
14 Supporting information (SI): SI includes humalog insulin composition, Contrast variation method details, SLDs, SANS result summary and SANS data analyses.
15 L. R. MacGillivray and J. L. Atwood, *Nature*, 1997, **389**, 469–472.
16 J. L. Atwood, L. J. Barbour, T. J. Ness, C. L. Raston and P. L. Raston, *J. Am. Chem. Soc.*, 2001, **123**, 7192–7193.
17 J. L. Atwood, L. J. Barbour and A. Jerga, *J. Supramol. Chem.*, 2002, **1**, 131–134.
18 S. J. Dalgarno, S. A. Tucker, D. B. Bassil and J. L. Atwood, *Science*, 2005, **309**, 2037–2039.
19 S. J. Dalgarno, D. B. Bassil, S. A. Tucker and J. L. Atwood, *Angew. Chem., Int. Ed.*, 2006, **45**, 7019–7022.
20 C. Bonaccorso, A. Ciadamidaro, C. Sgarlata, D. Sciotto and G. Arena, *Chem. Commun.*, 2010, **46**, 7139.
21 C. Bonaccorso, C. Sgarlata, G. Grasso, V. Zito, D. Sciotto and G. Arena, *Chem. Commun.*, 2011, **47**, 6117.
22 M. Makha, C. L. Raston, A. N. Sobolev and P. Turner, *Cryst. Growth Des.*, 2006, **6**, 224–228.
23 V. I. Timofeev, A. N. Baidus, Y. A. Kislitsyn and I. P. Kuranova, PDB Id: 3E7Z; To be published.
24 C. J. Glinka, J. G. Barker, B. Hammouda, S. Krueger, J. J. Moyer and W. J. Orts, *J. Appl. Crystallogr.*, 1998, **31**, 430–445.
25 S. R. Kline, *J. Appl. Crystallogr.*, 2006, **39**, 895–900.
26 G. V. Schulz, *Z. physik. Chem.*, 1935, **B30**, 379–398.
27 G. V. Schulz, *Z. physik. Chem.*, 1939, **B43**, 25–46.
28 H. Kumari, S. R. Kline, N. J. Schuster and J. L. Atwood, *Chem. Commun.*, 2011, **47**, 12298.
29 A. Nayak, M. Sorci, S. Krueger and G. Belfort, *Proteins: Struct., Funct., Bioinf.*, 2009, **74**, 556–565.
30 M. Kotlarchyk and S. H. Chen, *J. Chem. Phys.*, 1983, **79**, 2461–2469.
31 H. Kumari, A. V. Mossine, S. R. Kline, C. L. Dennis, D. A. Fowler, C. L. Barnes, S. J. Teat, C. A. Deakyne and J. L. Atwood, *Angew. Chem., Int. Ed.*, 2012, **51**, 1452–1454.
32 H. Kumari, S. R. Kline, N. J. Schuster, C. L. Barnes and J. L. Atwood, *J. Am. Chem. Soc.*, 2011, **133**, 18102–18105.